



Cite this: *Chem. Sci.*, 2021, 12, 14182

All publication charges for this article have been paid for by the Royal Society of Chemistry

Enantioselective palladaelectro-catalyzed C–H olefinations and allylations for N–C axial chirality†

Uttam Dhawa,^{‡a} Tomasz Wdowik,^{‡a} Xiaoyan Hou,^{‡a} Binbin Yuan,^a João C. A. Oliveira^{‡a} and Lutz Ackermann^{‡*ab}

Enantioselective palladaelectro-catalyzed C–H alkenylations and allylations were achieved with easily-accessible amino acids as transient directing groups. This strategy provided access to highly enantiomerically-enriched N–C axially chiral scaffolds under exceedingly mild conditions. The synthetic utility of our strategy was demonstrated by a variety of alkenes, while the versatility of our approach was reflected by atroposelective C–H allylations. Computational studies provided insights into a facile C–H activation by a seven-membered palladacycle.

Received 24th August 2021
Accepted 4th October 2021

DOI: 10.1039/d1sc04687j

rsc.li/chemical-science

Introduction

Organic electrocatalysis has surfaced as an increasingly powerful platform in the molecular sciences.¹ Despite indisputable advances, asymmetric electro-organic synthesis continues to be underdeveloped.² Particularly, the development of highly enantioselective electrocatalysis remains a challenge,³ while gaining full selectivity control is paramount for synthetically useful C–H transformations.⁴ In this context, we have recently developed the asymmetric metallaelectro-catalyzed C–H activation,⁵ largely leading to C–C axially chiral binaphthyls.⁶

N–C axially chiral heterobiaryls are key structural motifs in chiral catalysts, ligands, and natural products (Fig. 1a).^{7,8} Despite significant advances in the synthesis of chiral biaryls,⁹ the enantioselective assembly of N–C axially chiral molecules continues to be scarce.¹⁰ As a consequence, recent focus has shifted towards methods for the preparation of N–C axially chiral scaffolds, with key contributions by Wencel-Delord/Colobert,⁸ Xie¹¹ and Shi,¹² among others. However, the kinetic resolution with sterically-crowded *N*-arylindoles was restricted to the use of superstoichiometric amounts of toxic and cost-intensive silver salts in expensive fluorinated solvents, significantly jeopardizing the sustainability of the overall approach (Fig. 1b).¹¹ Within our program on sustainable C–H activations,¹³ we have now unraveled an electrochemical kinetic resolution¹⁴ of *N*-arylindoles in the presence of a transient directing group (TDG)¹⁵ (Fig. 1c).



N–C axially chiral scaffold
Asymmetric electrocatalytic C–H activation
No waste product
C–H allylation
Selectivity factors up to S = 355

Fig. 1 Evolution of electrocatalytic C–H activation towards N–C axial chirality. (a) Examples of N–C axially chiral compounds; (b) atroposelective palladacatalysis; (c) enantioselective metallaelectrocatalysis.

^aInstitut für Organische und Biomolekulare Chemie, Georg-August-Universität Göttingen, Tammannstraße 2, 37077 Göttingen, Germany. E-mail: Lutz.Ackermann@chemie.uni-goettingen.de

^bWöhler Research Institute for Sustainable Chemistry (WISCh), Georg-August-Universität Göttingen, Tammannstraße 2, 37077 Göttingen, Germany

† Electronic supplementary information (ESI) available. CCDC 2090275. For ESI and crystallographic data in CIF or other electronic format see DOI: 10.1039/d1sc04687j

‡ These authors contributed equally to this work.



Notable features of our findings include (a) enantioselective organometallic C–H activation¹⁶ for the electrocatalytic assembly of N–C axially chiral scaffolds in the absence of toxic chemical oxidants, (b) easily-accessible transient directing groups in electrochemical C–H activations, (c) a wide substrate scope of maleimides and fluorinated alkenes, and (d) key mechanistic insights by computation, (e) leading to atroposelective electrochemical C–H allylations.

Results and discussion

We initiated our studies with *L*-*tert*-leucine as additive for the envisioned atroposelective electrochemical kinetic resolution of racemic *N*-arylindoles **1** for the synthesis of N–C axially chiral motifs (Tables 1 and S1 in the ESI†).¹⁷ Hence, racemic indole **1a** was reacted with *n*-butyl acrylate (**2a**) in the presence of catalytic amounts of Pd(OAc)₂ and *L*-*tert*-leucine as well as LiOAc in AcOH at 60 °C to provide the desired alkene **3** with 97% ee, while the recovered starting material **1a** was obtained in 70% ee (entry 1). We were delighted to find that *L*-*tert*-leucine diethyl amide provided an excellent selectivity factor of *S* = 264, albeit at a lower conversion (entry 2). In contrast, *L*-proline provided the C3 alkenylated product, highlighting the challenges to overcome the innate C3 reactivity of indole.¹⁷ We did not observe reactivity, when TFE was used as the solvent (entry 3). Low conversions were obtained in a solvent mixture of TFE and AcOH (entry 4). Control experiments revealed the necessity of the TDG, and the palladium catalyst for the atroposelective electrochemical resolution of *N*-arylindole **1a** (entries 5–7), while electricity proved to be important for improving the



Fig. 2 On/off electricity experiment.

catalytic efficacy (Table S1†). Notably, the reaction worked efficiently under N₂ atmosphere, albeit with lower conversion (entry 8). However, the addition of benzoquinone as redox mediator failed to improve the conversion (entry 9). Thus, the metallaelectrocatalysis proceeded efficiently under mild conditions in redox-mediator-free condition.

On/off experiments clearly showed the essential role of the electricity to improve the efficacy of the electrocatalytic C–H activation (Fig. 2).

With the optimized reaction conditions in hand, we next explored the scope of the palladaelectro-catalyzed N–C atroposelective olefination (Scheme 1). Thus, a wide variety of alkenes **2** provided the desired products **3–11** with excellent selectivity factors (*S*). Specifically, *n*-butyl acrylate (**2a**) and *t*-butyl acrylate (**2b**) provided the desired olefinated products **3** and **4** with 97% ee and 92% ee, respectively. Vinyl phosphonate (**2c**) and vinyl sulfone (**2d**) were also identified as suitable substrates to deliver the desired products **5** and **6**, respectively, with high *S*-factors. An arene with an electron-donating methoxy group **2e** likewise performed well, providing the olefinated product **7** with 92% ee. The bromo-substituted arene **2f** was well tolerated in the N–C atroposelective alkenylation with an excellent *S*-factor of 355, which should prove invaluable for further late-stage modification. The palladaelectrocatalysis proceeded likewise with electron-rich 5-methyl substituted *N*-arylindole **1b** with a wide range of alkenes **2**. In contrast, unactivated alkenes gave thus far less satisfactory results, under otherwise identical conditions.

Maleimides represent key structural motifs in several natural products and drug candidates.¹⁸ Hence, we next examined the versatility of the N–C atroposelective transformations with maleimides **12** (Scheme 2). We were pleased to find that the robust electrocatalysis was viable for maleimides **12**. A variation of the substitution pattern on the nitrogen atom was explored, to give the methyl (**13**), cyclohexyl (**14**) and phenyl (**15**) substituted products with excellent *S*-factors. To our delight, *L*-*tert*-leucine diethyl amide provided the desired product **13** with an excellent *S*-factor of 272. The absolute configuration of product **15** was unambiguously assigned by X-ray diffraction analysis.

Table 1 Optimization of the N–C atroposelective C–H olefination^a

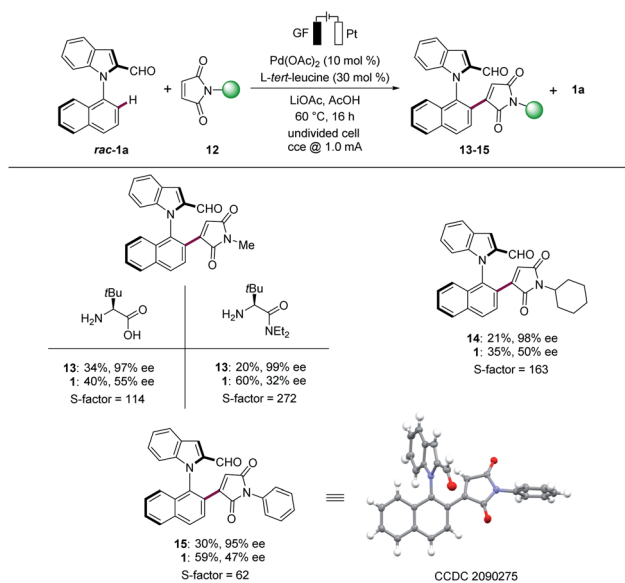
Entry	Deviation from standard conditions	Conv. ^b (%)	ee (3)	<i>S</i> ^c
1	None	42	97	138
2	<i>L</i> - <i>tert</i> -Leucine diethyl amide as TDG	23	99	264
3	TFE as solvent, no LiOAc	—	—	—
4	TFE/AcOH as solvent, no LiOAc	38	94	56
5	<i>L</i> - <i>tert</i> -Leucine (20 mol%)	37	97	118
6	No palladium	—	—	—
7	No <i>L</i> - <i>tert</i> -leucine	12 ^d	—	—
8	Under N ₂	26	99	280
9	1,4-Benzoquinone	36 ^e	99	347

^a Reaction conditions: undivided cell, *rac*-**1a** (0.20 mmol), **2a** (0.60 mmol), [Pd] (10 mol%), *L*-*tert*-leucine (30 mol%), LiOAc (2.0 equiv.), AcOH (4.5 mL), 60 °C, constant current at 1.0 mA, 16 h, graphite felt (GF) anode, Pt-plate cathode. ^b Calculated conversion, $C = ee_{1a}/(ee_{1a} + ee_3)$, $ee_{1a} = ee$ of **1a** and $ee_3 = ee$ of **3**. ^c Selectivity (*S*) = $\ln[(1 - C)/(1 - ee_{1a})]/\ln[(1 - C)/(1 + ee_{1a})]$. ^d C3 alkenylated product was isolated. ^e 1,4-Benzoquinone (10 mol%) as additive.





Scheme 1 N–C atroposelective C–H olefination of *N*-arylindoles *rac*-1.



Scheme 2 N–C atroposelective palladaelectro-catalyzed C–H olefination with maleimides **12**.

To gain insight into the N–C atroposelective C–H alkenylation, the reaction mechanism was probed by means of DFT calculations at the PW6B95-D4/def2-TZVP+SMD(AcOH)//PBE0-D3BJ/def2-SVP level of theory for the alkylation with maleimides **12** (Fig. 3).¹⁹ In the C–H activation step, both the pathways giving origin to the five- and seven-membered ring cyclometalated species were considered. Not only the intermediate **I-1** but also **TS(1-2)**, leading to the seven-membered



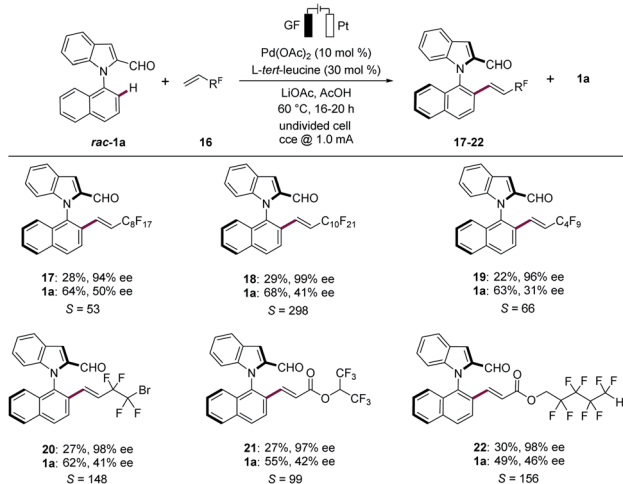
Fig. 3 Computed relative Gibbs free energies ($\Delta G_{333,15}$) in kcal mol⁻¹ between the C–H activation and insertion elementary steps at the PW6B95-D4/def2-TZVP+SMD(AcOH)//PBE0-D3BJ/def2-SVP level of theory. Superscripts 5 and 7 relate to structures, which lead to the formation of the 7-membered and the 5-membered cyclometalated intermediates.

cyclometalated complex revealed to be more favorable over the five-membered ring pathway by 6.7 and 2.3 kcal mol⁻¹ in **I-1** and **TS(1-2)**, respectively. Additionally, for the seven-membered ring pathway both the N- and O-coordination of the TDG to the palladium were considered. The O-coordinated pathway is strongly stabilized over the N-coordinated path by 13.1 and 11.4 kcal mol⁻¹ in **I-1** and **TS(1-2)** respectively. Thus, the C–H activation proceeds through an energetically preferred seven-membered ring pathway with a favored O-coordination of the TDG to the palladium in a facile fashion with a barrier of 12.6 kcal mol⁻¹. The C–H activation step is followed by the coordination of the maleimide giving origin to the formation of intermediate **I-4**, which undergoes migratory insertion through **TS(4-5)** with an energy barrier of 13.6 kcal mol⁻¹. These results indicate that C–H activation is not the rate determining-step.

Since the directed C3 position selectivity was observed with *l*-proline, the C–H activation elementary step was explored by computation (Fig. S5, see the ESI[†]).¹⁷ DFT calculations demonstrate that the C–H elementary step proceeded in a facile fashion at C3 of the indole with a low barrier of 18.2 kcal mol⁻¹. This barrier is higher than the one calculated for the cationic pathway (Fig. 3). This may be due to the presence of a hydrogen bond stabilization between the *l*-proline NH and the acetate in intermediate **I-1**^P, which needs to be disrupted upon acetate rotation, to give rise to transition state **TS(1-2)**^P.

Fluorinated organic compounds have gained considerable recent attention in pharmaceutical and agrochemical industries, among others, due to their improved lipophilicities.²⁰ Hence, we were pleased to find that the palladaelectro-catalyzed kinetic resolution proved to be amenable to fluorinated alkenes **16** for the synthesis of synthetically useful N–C axially chiral

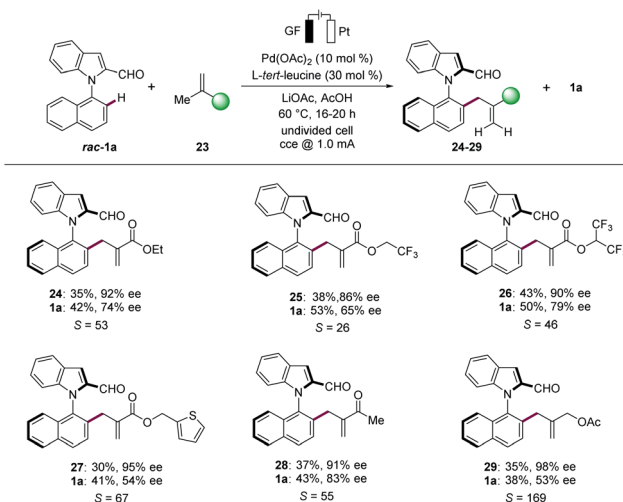




Scheme 3 N-C atroposelective palladaelectro-catalyzed C-H olefination with fluorinated alkenes **16**.

fluorinated motifs (Scheme 3). Thereby, various perfluorinated alkenes **16** provided the desired fluorinated compounds **17–22**. Likewise, terminal perfluoroalkylalkenes with different chain lengths **16a–16c** reflected the versatility with excellent selectivity factors. Interestingly, the presence of bromine in perfluoroalkylalkene **16d** did not alter the course of the electrocatalysis. Thus, the corresponding product **20** was obtained in 27% yield and 98% ee. Additionally, similar reactivities were observed when alkenes **16e** and **16f** were employed, providing the desired products **21** and **22** with *S*-factors of 99 and 156, respectively.

Finally, the N-C atroposelective electrocatalysis was not limited to monosubstituted alkenes. Indeed, unprecedented allylic selectivity²¹ was observed with 1,1-disubstituted alkenes²² for the synthesis of atroposelective N-C axially chiral heterobiaryls **24–29** (Scheme 4). The electrocatalysis proceeded



Scheme 4 N-C atroposelective palladaelectro-catalyzed C-H allylation.

efficiently with ethyl methacrylate (**23a**) to provide the corresponding product **24** with complete allylic selectivity in 35% yield and 92% ee. Similarly, fluorinated methacrylates **23b** and **23c** were found to be suitable substrates, providing the desired allylated products **25** and **26**, respectively, with high enantioselectivities. Importantly, thiophenyl methacrylate (**23d**) was also successfully explored. We were pleased to find that methyl butenone (**23e**) was efficiently converted, providing the allylation product **28** with 91% ee. The reactivity was not limited to 1,1-disubstituted alkenes conjugated with electron withdrawing groups, since methylallyl ester **23f** likewise delivered the allylated product **29** with high enantioselectivity.

Furthermore, we probed the electrochemical C-H olefination by means of cyclic voltammetric analysis (Fig. 4 and S2–S4†).¹⁷ The oxidation peak at 1.1 V vs. SCE appeared after the first negative sweep of Pd(OAc)₂, which corresponds to the oxidation of palladium(0) to palladium(II) (Fig. S2†). This redox event is significantly lower than the oxidation potential of the other components, being suggestive of the current regenerating the catalytically active palladium species (Fig. 4).

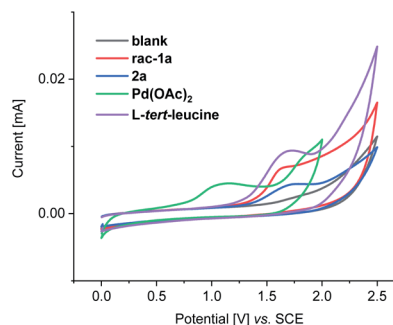


Fig. 4 Cyclic voltammogram of several reactants in AcOH with *n*Bu₄NPF₆ (0.1 M) at 100 mV s⁻¹.



Scheme 5 Proposed catalytic cycle.



Based on our experimental and computational findings, we proposed the N–C atroposelective palladaelectro-catalyzed C–H olefination to commence with the coordination of the *in situ* generated imine **1a'** with the palladium catalyst **A** leading to the formation of intermediate **B**, which subsequently undergoes facile C–H metalation (Scheme 5). Coordination of the alkene gives palladium allyl species **D** by migratory insertion, which is followed by β -H elimination to form complex **E**. The latter leads to the formation of a palladium(0) complex **F** which subsequently undergoes anodic oxidation to regenerate the palladium(II) catalytically active species **A**.²³

Conclusions

In summary, we have reported on the unprecedented atroposelective palladaelectro-catalyzed C–H activation for the synthesis of N–C axially chiral indole biaryls. The atroposelective organometallic C–H activation was realized by means of a chiral amino acid under mild conditions. Thus, N–C axially chiral scaffolds were obtained with good to excellent selectivity factors in the absence of chemical oxidants. A wealth of alkenes was found to be compatible with this strategy, including nonactivated and perfluorinated alkenes. The first N–C atroposelective palladium(II)-catalyzed C–H allylation was achieved with challenging 1,1-disubstituted alkene, while computational studies on the metallaelectrocatalysis unraveled a facile C–H activation.

Data availability

All experimental data, procedures for data analysis and pertinent data sets are provided in the ESI.†

Author contributions

U. D., T. W. and L. A. conceived the project. U. D., T. W. and X. H. performed the experiments. X. H. performed CV studies. B. Y. and J. C. A. O. performed DFT calculations. U. D. and L. A. wrote the manuscript. All of the authors discussed the results and contributed to the preparation of the final manuscript.

Conflicts of interest

There are no conflicts to declare.

Acknowledgements

Generous support by the DFG (Gottfried-Wilhelm-Leibniz award and SPP 1807), the DAAD (fellowship to U. D.), and the CSC (scholarships to X. H. and B. Y.) is gratefully acknowledged. The authors thank Dr Christopher Golz (University of Göttingen) for assistance with the X-ray diffraction analysis and Ms Agnese Zangarelli (University of Göttingen) for early experimentation and starting material synthesis.

Notes and references

- (a) L. F. T. Novaes, J. Liu, Y. Shen, L. Lu, J. M. Meinhardt and S. Lin, *Chem. Soc. Rev.*, 2021, **50**, 7941–8002; (b) C. Zhu, N. W. J. Ang, T. H. Meyer, Y. Qiu and L. Ackermann, *ACS Cent. Sci.*, 2021, **7**, 415–431; (c) D. Pollok and S. R. Waldvogel, *Chem. Sci.*, 2020, **11**, 12386–12400; (d) J. C. Siu, N. Fu and S. Lin, *Acc. Chem. Res.*, 2020, **53**, 547–560; (e) P. Xiong and H.-C. Xu, *Acc. Chem. Res.*, 2019, **52**, 3339–3350; (f) J.-i. Yoshida, A. Shimizu and R. Hayashi, *Chem. Rev.*, 2018, **118**, 4702–4730; (g) G. S. Sauer and S. Lin, *ACS Catal.*, 2018, **8**, 5175–5187; (h) K. D. Moeller, *Chem. Rev.*, 2018, **118**, 4817–4833; (i) M. Yan, Y. Kawamata and P. S. Baran, *Chem. Rev.*, 2017, **117**, 13230–13319; (j) R. Francke and R. D. Little, *Chem. Soc. Rev.*, 2014, **43**, 2492–2521; (k) T. R. Cook, D. K. Dogutan, S. Y. Reece, Y. Surendranath, T. S. Teets and D. G. Nocera, *Chem. Rev.*, 2010, **110**, 6474–6502; (l) J.-i. Yoshida, K. Kataoka, R. Horcajada and A. Nagaki, *Chem. Rev.*, 2008, **108**, 2265–2299; (m) A. Jutand, *Chem. Rev.*, 2008, **108**, 2300–2347.
- (a) T. H. Meyer, I. Choi, C. Tian and L. Ackermann, *Chem*, 2020, **6**, 2484–2496; (b) X. Chang, Q. Zhang and C. Guo, *Angew. Chem., Int. Ed.*, 2020, **59**, 12612–12622; (c) Q. Lin, L. Li and S. Luo, *Chem.–Eur. J.*, 2019, **25**, 10033–10044; (d) M. Ghosh, V. S. Shinde and M. Rueping, *Beilstein J. Org. Chem.*, 2019, **15**, 2710–2746.
- (a) S. G. Robinson, X. Wu, B. Jiang, M. S. Sigman and S. Lin, *J. Am. Chem. Soc.*, 2020, **142**, 18471–18482; (b) L. Song, N. Fu, B. G. Ernst, W. H. Lee, M. O. Frederick, R. A. DiStasio and S. Lin, *Nat. Chem.*, 2020, **12**, 747–754; (c) H. Qiu, B. Shuai, Y.-Z. Wang, D. Liu, Y.-G. Chen, P.-S. Gao, H.-X. Ma, S. Chen and T.-S. Mei, *J. Am. Chem. Soc.*, 2020, **142**, 9872–9878; (d) P.-S. Gao, X.-J. Weng, Z.-H. Wang, C. Zheng, B. Sun, Z.-H. Chen, S.-L. You and T.-S. Mei, *Angew. Chem., Int. Ed.*, 2020, **59**, 15254–15259; (e) X. Huang, Q. Zhang, J. Lin, K. Harms and E. Meggers, *Nat. Catal.*, 2019, **2**, 34–40; (f) T. J. DeLano and S. E. Reisman, *ACS Catal.*, 2019, **9**, 6751–6754; (g) N. Kise, Y. Hamada and T. Sakurai, *Org. Lett.*, 2014, **16**, 3348–3351; (h) N. Kise, H. Ozaki, N. Moriyama, Y. Kitagishi and N. Ueda, *J. Am. Chem. Soc.*, 2003, **125**, 11591–11596.
- (a) O. Vyhivskiy, A. Kudashev, T. Miyakoshi and O. Baudoin, *Chem.–Eur. J.*, 2021, **27**, 1231–1257; (b) T. K. Achar, S. Maiti, S. Jana and D. Maiti, *ACS Catal.*, 2020, **10**, 13748–13793; (c) G. Meng, N. Y. S. Lam, E. L. Lucas, T. G. Saint-Denis, P. Verma, N. Chekshin and J.-Q. Yu, *J. Am. Chem. Soc.*, 2020, **142**, 10571–10591; (d) G. Liao, T. Zhou, Q.-J. Yao and B.-F. Shi, *Chem. Commun.*, 2019, **55**, 8514–8523; (e) Ł. Woźniak and N. Cramer, *Trends Chem.*, 2019, **1**, 471–484; (f) J. Loup, U. Dhawa, F. Pescioli, J. Wencel-Delord and L. Ackermann, *Angew. Chem., Int. Ed.*, 2019, **58**, 12803–12818; (g) J. Diesel and N. Cramer, *ACS Catal.*, 2019, **9**, 9164–9177; (h) C. G. Newton, S.-G. Wang, C. C. Oliveira and N. Cramer, *Chem. Rev.*, 2017, **117**, 8908–8976; (i) D.-W. Gao, Q. Gu, C. Zheng and S.-L. You, *Acc. Chem. Res.*, 2017, **50**,



- 351–365; (j) J. Wencel-Delord, A. Panossian, F. R. Leroux and F. Colobert, *Chem. Soc. Rev.*, 2015, **44**, 3418–3430.
- 5 (a) R. C. Samanta, T. H. Meyer, I. Siewert and L. Ackermann, *Chem. Sci.*, 2020, **11**, 8657–8670; (b) K.-J. Jiao, Y.-K. Xing, Q.-L. Yang, H. Qiu and T.-S. Mei, *Acc. Chem. Res.*, 2020, **53**, 300–310; (c) P. Gandeepan, L. H. Finger, T. H. Meyer and L. Ackermann, *Chem. Soc. Rev.*, 2020, **49**, 4254–4272; (d) Y. Qiu, J. Struwe and L. Ackermann, *Synlett*, 2019, **30**, 1164–1173; (e) N. Sauermann, T. H. Meyer, Y. Qiu and L. Ackermann, *ACS Catal.*, 2018, **8**, 7086–7103; (f) N. Sauermann, T. H. Meyer and L. Ackermann, *Chem.–Eur. J.*, 2018, **24**, 16209–16217; (g) C. Ma, P. Fang and T.-S. Mei, *ACS Catal.*, 2018, **8**, 7179–7189; (h) M. D. Kärkäs, *Chem. Soc. Rev.*, 2018, **47**, 5786–5865.
- 6 U. Dhawa, C. Tian, T. Wdowik, J. C. A. Oliveira, J. Hao and L. Ackermann, *Angew. Chem., Int. Ed.*, 2020, **59**, 13451–13457.
- 7 T. Sugane, T. Tobe, W. Hamaguchi, I. Shimada, K. Maeno, J. Miyata, T. Suzuki, T. Kimizuka, S. Sakamoto and S.-i. Tsukamoto, *J. Med. Chem.*, 2013, **56**, 5744–5756.
- 8 J. Frey, A. Malekafzali, I. Delso, S. Choppin, F. Colobert and J. Wencel-Delord, *Angew. Chem., Int. Ed.*, 2020, **59**, 8844–8848.
- 9 (a) X. Wu, R. M. Witzig, R. Beaud, C. Fischer, D. Häussinger and C. Sparr, *Nat. Catal.*, 2021, **4**, 457–462; (b) B.-B. Zhan, L. Wang, J. Luo, X.-F. Lin and B.-F. Shi, *Angew. Chem., Int. Ed.*, 2020, **59**, 3568–3572; (c) H. Song, Y. Li, Q.-J. Yao, L. Jin, L. Liu, Y.-H. Liu and B.-F. Shi, *Angew. Chem., Int. Ed.*, 2020, **59**, 6576–6580; (d) L. Jin, Q.-J. Yao, P.-P. Xie, Y. Li, B.-B. Zhan, Y.-Q. Han, X. Hong and B.-F. Shi, *Chem*, 2020, **6**, 497–511; (e) Q. Wang, Z.-J. Cai, C.-X. Liu, Q. Gu and S.-L. You, *J. Am. Chem. Soc.*, 2019, **141**, 9504–9510; (f) J. Luo, T. Zhang, L. Wang, G. Liao, Q.-J. Yao, Y.-J. Wu, B.-B. Zhan, Y. Lan, X.-F. Lin and B.-F. Shi, *Angew. Chem., Int. Ed.*, 2019, **58**, 6708–6712; (g) G. Liao, H.-M. Chen, Y.-N. Xia, B. Li, Q.-J. Yao and B.-F. Shi, *Angew. Chem., Int. Ed.*, 2019, **58**, 11464–11468; (h) G. Liao, Q.-J. Yao, Z.-Z. Zhang, Y.-J. Wu, D.-Y. Huang and B.-F. Shi, *Angew. Chem., Int. Ed.*, 2018, **57**, 3661–3665; (i) G. Liao, B. Li, H.-M. Chen, Q.-J. Yao, Y.-N. Xia, J. Luo and B.-F. Shi, *Angew. Chem., Int. Ed.*, 2018, **57**, 17151–17155; (j) Q. Dherbassy, J.-P. Djukic, J. Wencel-Delord and F. Colobert, *Angew. Chem., Int. Ed.*, 2018, **57**, 4668–4672; (k) Q.-J. Yao, S. Zhang, B.-B. Zhan and B.-F. Shi, *Angew. Chem., Int. Ed.*, 2017, **56**, 6617–6621; (l) J. Zheng, W.-J. Cui, C. Zheng and S.-L. You, *J. Am. Chem. Soc.*, 2016, **138**, 5242–5245; (m) Q. Dherbassy, G. Schwertz, M. Chessé, C. K. Hazra, J. Wencel-Delord and F. Colobert, *Chem.–Eur. J.*, 2016, **22**, 1735–1743; (n) J. Zheng and S.-L. You, *Angew. Chem., Int. Ed.*, 2014, **53**, 13244–13247; (o) C. K. Hazra, Q. Dherbassy, J. Wencel-Delord and F. Colobert, *Angew. Chem., Int. Ed.*, 2014, **53**, 13871–13875; (p) T. Wesch, F. R. Leroux and F. Colobert, *Adv. Synth. Catal.*, 2013, **355**, 2139–2144.
- 10 (a) J. K. Cheng, S.-H. Xiang, S. Li, L. Ye and B. Tan, *Chem. Rev.*, 2021, **121**, 4805–4902; (b) A. Link and C. Sparr, *Chem. Soc. Rev.*, 2018, **47**, 3804–3815; (c) B. Zilate, A. Castrogiovanni and C. Sparr, *ACS Catal.*, 2018, **8**, 2981–2988; (d) J. Wencel-Delord and F. Colobert, *Synthesis*, 2016, **48**, 2981–2996.
- 11 J. Zhang, Q. Xu, J. Wu, J. Fan and M. Xie, *Org. Lett.*, 2019, **21**, 6361–6365.
- 12 (a) Y.-J. Wu, P.-P. Xie, G. Zhou, Q.-J. Yao, X. Hong and B.-F. Shi, *Chem. Sci.*, 2021, **12**, 9391–9397; (b) Q.-J. Yao, P.-P. Xie, Y.-J. Wu, Y.-L. Feng, M.-Y. Teng, X. Hong and B.-F. Shi, *J. Am. Chem. Soc.*, 2020, **142**, 18266–18276; (c) S. Zhang, Q.-J. Yao, G. Liao, X. Li, H. Li, H.-M. Chen, X. Hong and B.-F. Shi, *ACS Catal.*, 2019, **9**, 1956–1961.
- 13 (a) L. Ackermann, *Acc. Chem. Res.*, 2020, **53**, 84–104; (b) L. Ackermann, *Acc. Chem. Res.*, 2014, **47**, 281–295.
- 14 M. R. Maddani, J.-C. Fiaud and H. B. Kagan, in *Separation of Enantiomers: Synthetic Methods* ed. M. Todd, Wiley-VCH, Weinheim, 2014, pp. 13–74.
- 15 (a) G. Liao, T. Zhang, Z.-K. Lin and B.-F. Shi, *Angew. Chem., Int. Ed.*, 2020, **59**, 19773–19786; (b) P. Gandeepan and L. Ackermann, *Chem*, 2018, **4**, 199–222; (c) Q. Zhao, T. Poisson, X. Pannecoucke and T. Besset, *Synthesis*, 2017, **49**, 4808–4826.
- 16 (a) T. Rogge, N. Kaplaneris, N. Chatani, J. Kim, S. Chang, B. Punji, L. L. Schafer, D. G. Musaev, J. Wencel-Delord, C. A. Roberts, R. Sarpong, Z. E. Wilson, M. A. Brimble, M. J. Johansson and L. Ackermann, *Nat. Rev. Dis. Primers*, 2021, **1**, 43; (b) U. Dhawa, N. Kaplaneris and L. Ackermann, *Org. Chem. Front.*, 2021, **8**, 4886–4913; (c) S. Rej, Y. Ano and N. Chatani, *Chem. Rev.*, 2020, **120**, 1788–1887; (d) A. Dey, S. K. Sinha, T. K. Achar and D. Maiti, *Angew. Chem., Int. Ed.*, 2019, **58**, 10820–10843; (e) Y. Park, Y. Kim and S. Chang, *Chem. Rev.*, 2017, **117**, 9247–9301; (f) J. He, M. Wasa, K. S. L. Chan, Q. Shao and J.-Q. Yu, *Chem. Rev.*, 2017, **117**, 8754–8786; (g) S. Agasti, A. Dey and D. Maiti, *Chem. Commun.*, 2017, **53**, 6544–6556; (h) O. Daugulis, J. Roane and L. D. Tran, *Acc. Chem. Res.*, 2015, **48**, 1053–1064; (i) G. Rouquet and N. Chatani, *Angew. Chem., Int. Ed.*, 2013, **52**, 11726–11743; (j) D. A. Colby, A. S. Tsai, R. G. Bergman and J. A. Ellman, *Acc. Chem. Res.*, 2012, **45**, 814–825; (k) L. Ackermann, R. Vicente and A. R. Kapdi, *Angew. Chem., Int. Ed.*, 2009, **48**, 9792–9826.
- 17 For detailed information, see supporting information†
- 18 (a) E. M. Sletten and C. R. Bertozzi, *Angew. Chem., Int. Ed.*, 2009, **48**, 6974–6998; (b) C. Peifer, T. Stoiber, E. Unger, F. Totzke, C. Schächtele, D. Marmé, R. Brenk, G. Klebe, D. Schollmeyer and G. Dannhardt, *J. Med. Chem.*, 2006, **49**, 1271–1281; (c) P. Sellès, *Org. Lett.*, 2005, **7**, 605–608.
- 19 (a) E. Caldeweyher, S. Ehlert, A. Hansen, H. Neugebauer, S. Spicher, C. Bannwarth and S. Grimme, *J. Chem. Phys.*, 2019, **150**, 154122; (b) S. Grimme, S. Ehrlich and L. Goerigk, *J. Comput. Chem.*, 2011, **32**, 1456–1465; (c) S. Grimme, J. Antony, S. Ehrlich and H. Krieg, *J. Chem. Phys.*, 2010, **132**, 154104; (d) F. Weigend, *Phys. Chem. Chem. Phys.*, 2006, **8**, 1057–1065; (e) Y. Zhao and D. G. Truhlar, *J. Phys. Chem. A*, 2005, **109**, 5656–5667; (f) F. Weigend and R. Ahlrichs, *Phys. Chem. Chem. Phys.*, 2005, **7**, 3297–3305; (g) J. M. L. Martin and A. Sundermann, *J. Chem. Phys.*, 2001, **114**, 3408–3420; (h) M. Ernzerhof and G. E. Scuseria, *J. Chem. Phys.*, 1999, **110**, 5029–5036; (i)



- C. Adamo and V. Barone, *J. Chem. Phys.*, 1999, **110**, 6158–6170; (j) A. Schäfer, C. Huber and R. Ahlrichs, *J. Chem. Phys.*, 1994, **100**, 5829–5835; (k) A. Schäfer, H. Horn and R. Ahlrichs, *J. Chem. Phys.*, 1992, **97**, 2571–2577; (l) M. Dolg, U. Wedig, H. Stoll and H. Preuss, *J. Chem. Phys.*, 1987, **86**, 866–872.
- 20 (a) T. Furuya, A. S. Kamlet and T. Ritter, *Nature*, 2011, **473**, 470–477; (b) K. Müller, C. Faeh and F. Diederich, *Science*, 2007, **317**, 1881–1886.
- 21 (a) S. Dutta, T. Bhattacharya, D. B. Werz and D. Maiti, *Chem*, 2021, **7**, 555–605; (b) U. Dhawa, C. Tian, W. Li and L. Ackermann, *ACS Catal.*, 2020, **10**, 6457–6462; (c) A. Baccalini, S. Vergura, P. Dolui, S. Maiti, S. Dutta, S. Maity, F. F. Khan, G. K. Lahiri, G. Zanoni and D. Maiti, *Org. Lett.*, 2019, **21**, 8842–8846; (d) T. K. Achar, X. Zhang, R. Mondal, M. S. Shanavas, S. Maiti, S. Maity, N. Pal, R. S. Paton and D. Maiti, *Angew. Chem., Int. Ed.*, 2019, **58**, 10353–10360; (e) T. Yamaguchi, Y. Kommagalla, Y. Aihara and N. Chatani, *Chem. Commun.*, 2016, **52**, 10129–10132; (f) S. Maity, P. Dolui, R. Kancherla and D. Maiti, *Chem. Sci.*, 2017, **8**, 5181–5185; (g) S. Maity, R. Kancherla, U. Dhawa, E. Hoque, S. Pimparkar and D. Maiti, *ACS Catal.*, 2016, **6**, 5493–5499; (h) G. Cera, T. Haven and L. Ackermann, *Angew. Chem., Int. Ed.*, 2016, **55**, 1484–1488.
- 22 B.-B. Zhan, Z.-S. Jia, J. Luo, L. Jin, X.-F. Lin and B.-F. Shi, *Org. Lett.*, 2020, **22**, 9693–9698.
- 23 C. Amatore, C. Cammoun and A. Jutand, *Adv. Synth. Catal.*, 2007, **349**, 292–296.

